Environ Biol Fish (2021) 104:1593–1610
https://doi.org/10.1007/s10641-021-01181-w

Ontogenetic development, allometric growth patterns, and daily increment validation of larvae and juvenile *Culter alburnus*

Yan F. Huang · Bo L. Song · Tao H. Deng · Qin Wang · Qi Shen · Liang G. Liu

Received: 12 April 2021 / Accepted: 18 October 2021 / Published online: 4 November 2021

Abstract Fish ontogeny, allometric growth patterns, and otolith microstructure are fundamental in aquaculture and essential for understanding the early-life ecology of fish. *Culter alburnus* is a commercially important fish species and an excellent breeding target for aquaculture. In this study, newly hatched *C. alburnus* larvae were reared to the juvenile stage in a hatchery. Three days post hatch, the eyes, mouth, and intestine had developed, and the larval yolk sac had been completely absorbed. Fin rays started to differentiate in the flexion stage and were fully developed by the postflexion stage. Pigmentations were well developed in the juveniles. *Culter alburnus* larvae were characterized by 39–43 myomeres and 23–25 anal fin rays, swim bladder shape, and pigmentation. Head length, height, and musculature height showed positive allometric growth patterns, suggesting that head and trunk growth was prioritized. Positive allometric growth of the tail was simultaneous with the formation of fins, suggesting that swimming mode transformation, diet changes, and habitat shifts occurred after the start of the postflexion stage. Otolith growth increments in both the sagittae and lapilli were deposited daily, with the first increment formed on day 1 on the sagittae and day 4 of yolk sac absorption on the lapilli. Increments were thin and faint during the early developmental stage, gradually increasing to reach the broadest widths and the strongest contrast at the postflexion stage, which may be related to habitat shifts. This information will assist in the breeding and hatchery production of *C. alburnus* and establish suitable methods for analyzing this species' spatiotemporal distributions and early-life traits.

Keywords Allometric growth · *Culter alburnus* · Cyprinidae · Ontogenetic development · Otoliths

Y. F. Huang (✉) · B. L. Song · L. G. Liu
College of Life and Environmental Science, Hunan University of Arts and Science, Dongting Main Street 3150, Wuling District, Changde, China
e-mail: hyf1221@163.com

Y. F. Huang · B. L. Song
Collaborative Innovation Center for Efficient and Health Production of Fisheries, Hunan University of Arts and Science, Dongting Main Street 3150, Wuling District, Changde, Hunan Province, China

T. H. Deng · Q. Wang · Q. Shen
Key Laboratory of Health Aquaculture and Product Processing in Dongting Lake Area of Hunan Province, Dongting Main Street 3150, Wuling District, Changde, China

Introduction

Annual recruitment in fish and adult populations can be determined during the early stages of their life history and is therefore important for fisheries management and habitat conservation (Houde 1987; Takahashi and Watanabe 2004; Shoji and Tanaka 2007). Research on the early life history of fish includes two integral parts: (1) abundance and spatiotemporal distribution of fish larvae and (2) growth and survival rates during

early life history stages (Belchier and Lawson 2013; Beveren et al. 2016). Knowledge of fish ontogeny and morphological characteristics allows for the identification of larval species and the analysis of abundance and spatiotemporal distribution of fish larvae (Koumoundouros et al. 1999; Rocha et al. 2020; dos Santos et al. 2020).

During ontogeny, larvae, which have an incomplete functional system, develop into juveniles within a short period (approximately 30 days) and undergo dramatic changes in body shape, morphology, metabolism, locomotion style, abilities, and respiration (Gisbert et al. 2002; Song et al. 2019). To adapt to environmental conditions, larval fish prioritize the development of essential organs and systems involved in feeding and locomotion, which increases their growth and survival rates (Peña and Dumas 2009; Khemis et al. 2013). This preferential development of organs results in allometric growth during ontogeny, which shows differences in relative growth rates among body parts and is expressed by plotting the size of individual body parts against body size. Allometric growth patterns lead to both fixed and phenotypically plastic morphological differences, which result in variable identification characteristics during different developmental stages (Gisbert 2002; Khemis et al. 2013; Saemi-Komsari et al. 2018). Therefore, studying early ontogeny and allometric growth patterns is not only helpful in understanding the environmental preferences of the different developmental stages and the spatial distribution of young fish but also indispensable for the assessment and optimization of hatchery production and rearing protocols (Koumoundouros et al. 1999; Sarpédonti et al. 2000; Saemi-Komsari et al. 2018).

Otolith microstructure is a critical tool for determining age and estimating fish growth and survival rate during early life history stages (Green et al. 2009). Fish have three otolith pairs, of which the sagitta and lapillus are usually present before hatching. Sagittae and lapilli are initially circular and change shape with ontogenetic development (Yan et al. 2017; Sanjarani et al. 2018; Bounket et al. 2019). Validation of daily increments and understanding the timing of deposition of the first increment are prerequisites for using otolith microstructure to study the early life history of fish (Huang et al. 2017; Bounket et al. 2019). Increment deposition, which is influenced by environmental conditions, typically occurs once per day under favorable environmental conditions but may cease under severe conditions of starvation or low temperature (Geffen 1982; Aldanondo et al. 2008). The first increment can be laid down during the embryonic period, hatching, yolk sac absorption, or first feeding, depending on the species (Hare and Cowen 1994; Green et al. 2009). Otolith microstructure characteristics are related to the physiological state, habitat type, and environmental stress. The otoliths can record major life history events, such as hatching, yolk sac absorption, first feeding, metamorphosis, and settlement, by forming corresponding marks, bands, or checks in the otoliths (Marannu et al. 2017; Bounket et al. 2019). Increment patterns also show variable widths and contrast at different developmental stages (Hernández et al. 2015; Huang et al. 2017). Determining the otolith microstructure and increment deposition rate is a basic requirement for understanding early life history traits and ascertaining the survival and recruitment success of young fish.

Culter alburnus Basilewsky 1855 is the largest fish in its genus, growing up to 10 kg in weight and 80 cm in length, and living for up to 11 years (Yin and Lv 2004). It is widely distributed throughout China between Taiwan in the south and Heilongjiang in the north, although it is most common in central and northern China. *Culter alburnus* is common in rivers and lakes, preferring lentic and slow-flowing habitats, and is often the dominant species in lakes, reservoirs, and impoundments (Huang et al. 2019). It is a predatory, piscivorous fish that mainly preys on small fish inhabiting the mid- and upper-water columns (Chiu et al. 2012). Because of the quality and taste of its meat, it has a high market value and supports an important commercial fishery; however, there have been substantial decreases in population size within most lakes and rivers due to overfishing and environmental degradation (Yin and Lv 2004; Liu et al. 2012; Dong et al. 2017). These factors make *C. alburnus* is an excellent breeding target for aquaculture.

Previous studies on the early life history of this species have focused on embryonic and early development. The embryonic developmental process has been described in great detail and compared among different populations in different rivers and lakes (Liu et al. 2012; Shao et al. 2016; Dong et al. 2017). Early development 1 to 4 days post hatch (dph) has been presented in some studies (Liu et al. 2012; Shao

et al. 2016), and morphological characteristics of larvae and juveniles have been reported by Gu et al. (2008). However, major morphological identification features and allometric growth patterns still need to be determined during their early life history. The age and growth of wild *C. alburnus* juveniles in the Three Gorges Reservoir have been estimated using otolith microstructure, based on the criteria for determining the age of validated Cyprinidae fish (Zhu et al. 2015). The validation of daily increments and the description of otolith microstructure development in *C. alburnus* are needed to further study the early life history traits of this species.

This study analyzed the ontogenetic development, growth patterns, and otolith microstructure of *C. alburnus* by rearing fish from hatching until juvenile at 53 dph. Larval and juvenile development are described in detail, emphasizing the characteristics that can be used to identify the early life stages of this species. Allometric growth patterns were determined to test the hypothesis that growth is prioritized in body parts related to feeding, respiration, and locomotion. In addition, the daily periodicity of increment formation was validated, the timing of the first increment was determined, and otolith increment patterns were observed throughout the developmental stages.

Materials and methods

Fish reared in the hatchery

Fertilized eggs were obtained by artificial breeding on May 24, 2018, in the Dongting Lake Fish Breeding Farm in Hunan, China. Eggs were incubated in a 5.6 × 1.4-m spawning pool that had continuously aerated flowing water. Larvae were hatched on May 25, 2018, and were moved into a recirculation system with circular pools (4 m diameter). After 3 days, the larvae had completely absorbed their yolk sac and were transferred into a pond and fed on the plankton living in the pond. The recirculation systems for both egg incubation and larvae rearing were operated under natural illumination and ambient water temperature, ranging from 25.1 to 28.0 °C (mean, 26.3 ± 1.06 °C) during the rearing periods. Fish were sampled daily from day 0 to 4 dph and then every 5th day until June 23, 2018.

Fish reared in the experimental center

Newly hatched larvae were brought back to the experimental center at Hunan University of Arts and Sciences on May 25, 2018. The larvae were reared in a 375 L rectangular tank at 28.0 ± 5.3 °C (23.0–32.1 °C), pH of 8.40 ± 0.37 (8.03–8.96), dissolved oxygen of 7.51 ± 2.09 (5.42 –8.37) mg/l, and under a natural photoperiod. Larvae were fed twice a day with egg yolk from 4 to 10 dph, then with shelled shrimp eggs until 25 dph, and after that, with a formulated feed (Tongwei Group Limited Company) until the end of the rearing period (52 dph). A large number of larvae (approximately 2/3) died at 3 dph due to the failure of the first feeding; after that, larval mortality rates were very low (approximately 1%). Waste and dead larvae were cleaned daily, and 1/3 of the water in the tank was replaced with fresh aerated water. At least 20 randomly selected larvae were sampled daily for the first 5 days, then every other day up to 23 dph, and after that, at 5-day intervals until the end of the experiment. These larvae were firstly euthanized with a lethal dose of eugenol and fixed in a 4% buffered formalin solution. After 2 h, half of the larvae were transferred to 85% neutral ethanol for otolith analysis. The remaining larvae were preserved in formalin solution for morphological observations.

Morphological observations and measurements

Each fish was observed under a Leica M205 stereo-zoom microscope (Leica Microsystems, Wetzlar, Germany) and photographed from its left side using digital image analysis software. According to Miller and Kendall (2009), developmental stages were identified as yolk sac, preflexion, flexion, postflexion larvae, and juveniles. Morphological characteristics, including yolk sac, eyes, pigmentation, mouth and anus openings, notochord flexion, swim bladder and intestine, finfolds, and fins, were recorded for each fish. Meristic traits were counted, including predorsal myomeres originating from the trunk to the dorsal finfold/fin, middle myomeres between the dorsal finfold/fin and the anus, the postanal myomeres from the anus to the end of the trunk, the pectoral, dorsal, anal, and pelvic fin rays. Morphometric traits (total length, body length [*BL*], body height, head length and height, eye diameter,

trunk length, musculature height, tail length, caudal peduncle length, snout length, predorsal length, preanal length, and pre-pelvic length) were measured to the nearest 0.01 mm from the pictures using the Image-Pro Plus program 6.0. These measurements followed dos Santos et al. (2020) and Song et al. (2019), except that total length was measured from the snout tip to the end of the caudal fin and caudal peduncle length measured from the anus to the caudal fin base. Morphometric variables are presented as a percentage of body length, except for eye diameter and snout length, which are presented as a percentage of head length. Additionally, the length and height of the yolk sac were measured, and the volume was calculated as $0.17 \times \pi \times \text{length} \times \text{height}^2$. The ontogenetic stage was defined as the duration from the smallest to the maximum *BL* of the given stage. The median size at the transition between two adjacent stages was calculated as the midpoint between the largest size of the previous developmental stage and the smallest size of the later stage (Huang et al. 2014).

The relationship between *BL* (mm) and age (days) was fitted to a Gompertz growth model:

$$BL = BL\infty e^{-e^{-k(t-t_f)}}$$

where t is the age at days, *BL* is the bode size at age t, t_f is the age at the inflection point of the curve, k is the instantaneous rate of growth, and BL_∞ is the asymptotic length.

Allometric growth patterns were modeled using a power function: $Y = aX^b$, where Y is the dependent variable (measured characters), X is the *BL*, a is the intercept, and b is the growth coefficient. Growth was isometric when $b = 1$, positively allometric when $b > 1$, and negatively allometric when $b < 1$ (Saemi-Komsari et al. 2018). The model was first calculated from piecewise linear regressions performed on log-transformed data to calculate the inflection point. Two linear regressions in the piecewise linear regression were established for 1) BL_{min} to $BL_{\text{intermediate}}$ and 2) $BL_{\text{intermediate}}$ to BL_{max}. Then a t-test was used to determine whether the two regression slopes were significantly different. The $BL_{\text{intermediate}}$ value, which ranged from $BL_{\text{min}} + 2$ to $BL_{\text{max}} - 2$, was defined as the inflection point when the comparison iteratively showed the largest t (Peña and Dumas 2009; van Snik et al. 1997).

Otolith preparation and validation of daily increments

Larvae stored in neutral ethanol shrank more than larvae stored in formalin, with smaller larvae having a higher shrinkage percentage. For example, larvae with $BL \leq 12$ mm that were stored in ethanol were $27.4 \pm 3.3\%$ (15.8–37.2%) shorter in *BL* compared to larvae stored in formalin, while larvae > 12 mm that were stored in ethanol were $3.4 \pm 5.6\%$ (1.0–12.9%) shorter in *BL* than in compared to larvae stored in formalin.

A pair of sagittae and a pair of lapilli were extracted from each specimen under a stereoscope, rinsed, dried, and mounted on a glass microscope with colorless nail varnish. Asterisci did not appear until the flexion stage and were excluded from further otolith analysis. Otolith microstructure traits were observed, counted and measured to the nearest 0.01 μm using an image analysis system (Jiseki ARP/W version 5.20, Ratoc System Engineering Company, Tokyo) with a direct data feed between an Olympus BX51 light microscope and a computer. The otolith length and otolith width were measured for each sagitta and lapillus. The otolith radius was measured from the core to the posterior edge of the otoliths parallel to the anterior–posterior axis. The number of increments was counted, and the width of each increment was measured along the otolith radius. Clear and readable increments appeared in the unpolished lapilli until the juvenile stage; after that, otoliths needed grinding using 3000 grit wet sandpaper and polished with 0.3-μm lapping film. The left or right otolith was randomly selected for analysis, and each selected otolith was counted independently twice by the same author. In this analysis, the mean of the two counts was used when the coefficient of variation of the two counts was $< 10\%$. The outermost light zone on the otoliths was excluded from the increment counts and increment width analyses. The day of sample collection was excluded when calculating the actual age of the fish.

Linear regression, quadratic function, and power functions were fitted to the length-at-radius data. The best model fit was assessed by comparing the coefficients of determination (r^2) and the residual sum of squares. As a result, the *BL*-at-radius relationship for the sagittae was best described by a quadratic function, whereas a linear regression best described the *BL*-at-radius relationship of the

lapilli. The relationship between the number of increments and the actual age was determined using a linear regression, of which the intercept corresponded to the day when the first increment formed, and the slope implied the increment periodicity. A *t*-test was used to determine whether the slope of the regression was significantly different from 1. All data are expressed as the mean ± standard deviation (*SD*), and the significance level was set at $P < 0.05$. All statistical analyses were performed using SPSS (version 16.0; SPSS Inc., Chicago, IL, USA) and STATISTICA 10.0 (TIBCO Software, Inc.).

Results

Growth under different rearing conditions

Larvae grew significantly faster in the hatchery than in the experimental tank from 8 dph (Fig. 1; Table 1). The Gompertz growth models had different parameter values of $L\infty = 59.03$ and 43.73, $K = 0.0426$ and 0.0232, and $tf = 21.95$ and 30.08 for hatchery ($n = 83$, $r2 = 0.97$) and for experimental larvae ($n = 151$, $r2 = 0.97$), respectively.

Ontogenetic development

Yolk-sac larva (Fig. 2a)

This stage lasted from hatching to 3 dph under both rearing conditions. Newly hatched larvae varied between 5.56 and 5.85 mm *BL* (mean ± *SD* = 5.72 ± 0.12 mm). At hatching (0 dph), the larva had a claviform yolk sac with an inflated anterior section, a length of 3.48 ± 0.13 mm (63.8% of *BL*), and a volume of 0.91 ± 0.14 mm^3. The head was bent downward, the mouth was closed, and the spherical eyes were unpigmented. The ventral and dorsal finfolds were confluent through the tail (Table 1), and the transparent body had a myomere count of 32–33.

At 1 dph, the head straightened, and one black spot appeared at the bottom of each eye. The yolk sac was sharply absorbed in the anterior section, with a volume of 0.65 ± 0.15 mm^3. Myomere counts varied from 37 to 42.

At 2 dph, the mouth opened and was in a subinferior position. The eyes were pigmented, and most of the yolk sac was depleted, with a length of 3.24 ± 0.22 mm (46.1% of *BL*) and a volume of 0.47 ± 0.11 mm^3. In addition, a slender intestinal tract adherent to the yolk sac appeared. Myomere counts varied from 39 to 42.

At 3 dph, the remnant yolk sac had a volume of 0.08 ± 0.04 mm^3. The intestine became thick, the

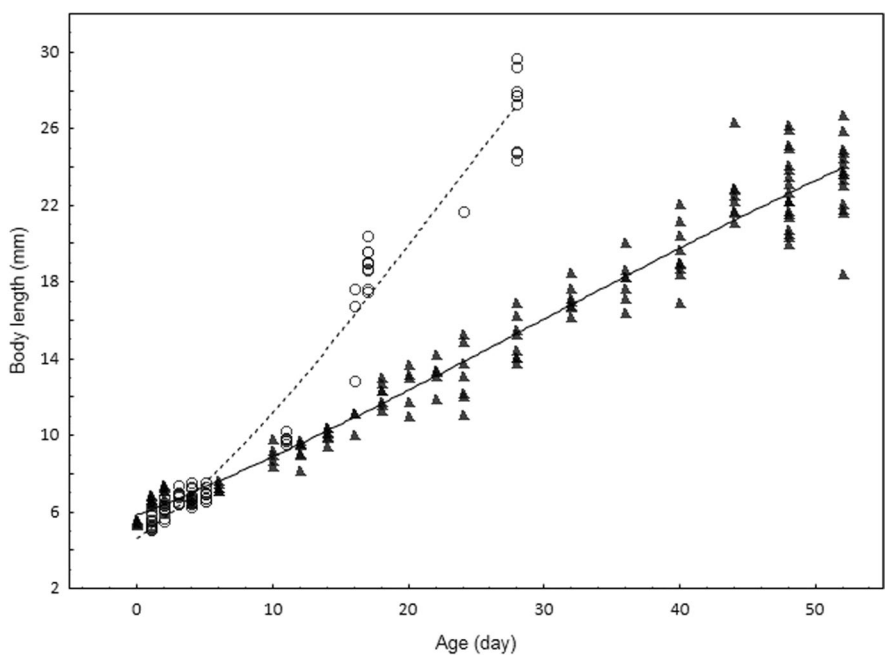

Fig. 1 The relationship between body length (mm) and days post hatching (dph) of *Culter alburnus* reared in the hatchery (circles) and the experimental tanks (triangles)

Table 1 Range of days post hatch and body size at each developmental stage and mean ± standard deviation (SD) for morphometric and meristic variables in larvae and juveniles of reared *Culter alburnus*

Variables	Developmental stages				
	Yolk-sac	Preflexion	Flexion	Postflexion	Juvenile
Rearing	Day post hatch (range)				
Experimental	0–3	4–12	10–24	22–28	28–52
Hatchery	0–3	4–10	8–17	15–17	17–30
Body size	Range, mm				
TL	5.56–7.86	6.71–9.77	9.52–16.19	15.76–20.06	20.37–36.61
BL	5.31–7.375	6.39–9.21	8.98–13.71	12.82–16.22	16.18–29.72
Relations	%, mean ± *SD* and range				
HL/BL	19.81 ± 0.86	21.10 ± 1.04	25.23 ± 1.66	28.02 ± 0.86	27.66 ± 0.90
	18.16–20.97	18.39–23.24	22.14–28.21	26.41–29.93	25.37–29.9
TrL/BL	47.23 ± 0.79	46.63 ± 1.52	43.68 ± 1.83	39.24 ± 1.34	36.80 ± 1.71
	46.11–48.22	43.67–49.44	39.53–49.59	37.28–42.13	33.85–41.53
CpL/BL	32.23 ± 0.95	33.22 ± 1.74	31.74 ± 2.27	31.68 ± 0.92	34.67 ± 1.39
	31.22–34.06	30.14–36.63	27.72–36.45	30.25–33.73	31.23–37.92
SnL/HL	14.17 ± 1.49	16.50 ± 3.54	20.64 ± 3.86	23.49 ± 1.86	25.56 ± 2.73
	12.33–16.49	13.44–18.58	15.72–26.7	22.19–25.73	19.11–28.19
ED/HL	26.60 ± 2.29	26.01 ± 3.17	25.72 ± 1.69	28.58 ± 1.47	31.15 ± 2.28
	22.47–31.48	20.29–33.04	23.58–31.61	25.64–30.94	25.43–36.82
PdL/BL	45.40 ± 5.00	45.20 ± 0.04	44.80 ± 2.20	42.30 ± 1.00	39.10 ± 2.50
	40.20–58.60	38.30–51.60	36.70–48.30	40.51–44.10	35.10–51.11
PaL/BL	NV	NV	70.46 ± 2.61	68.71 ± 1.42	66.21 ± 1.64
			68.99–79.19	67.05–71.67	61.26–70.92
PpL/BL	NV	NV	46.93 ± 0.88	47.14 ± 1.51	46.79 ± 2.34
			45.33–48.01	45.04–50.92	44.42–64.58
Rays					
P	NV	NV	NV	0–10	I, 11–15
V	NV	NV	NV	II, 0–8	II, 8
D	NV	NV	III, 0–7	III, 7	III, 7
A	NV	NV	III, 0–12	III, 10–22	III, 21–24
Myomere counts			≤/> 11 mm *BL*		
Total	32–42	39–42	40–44	NV	NV
Predorsal	11−12	11−13	11−12/13−15	NV	NV
Middle	11−12	11−13	11−13/9−11	NV	NV
Post-anal	16−18	16−18	17−18/18−20	20–22	NV

TL total length, *BL* body length, *HL* head length, *TrL* trunk length, *CpL* caudal peduncle length, *SnL* snout length, *PdL* predorsal length, *PpL* prepelvic length, *PaL* preanal length, *ED* eye diameter, *P* ray of the pectoral fin, *V* ray of the pelvic fin, *D* ray of the dorsal fin, *A* ray of the anal fin

anus opened, and active exogenous feeding was initiated. The intestinal finfold and anal finfold were separated, and a pair of pectoral fin buds appeared (Fig. 3). Predorsal, middle, and postanal myomeres were counted (Table 1).

Preflexion stage (Fig. 2b)

At 4 dph, an oval-shaped swimming bladder was inflated and increased in size throughout this stage. The forepart of the intestine gradually expanded and

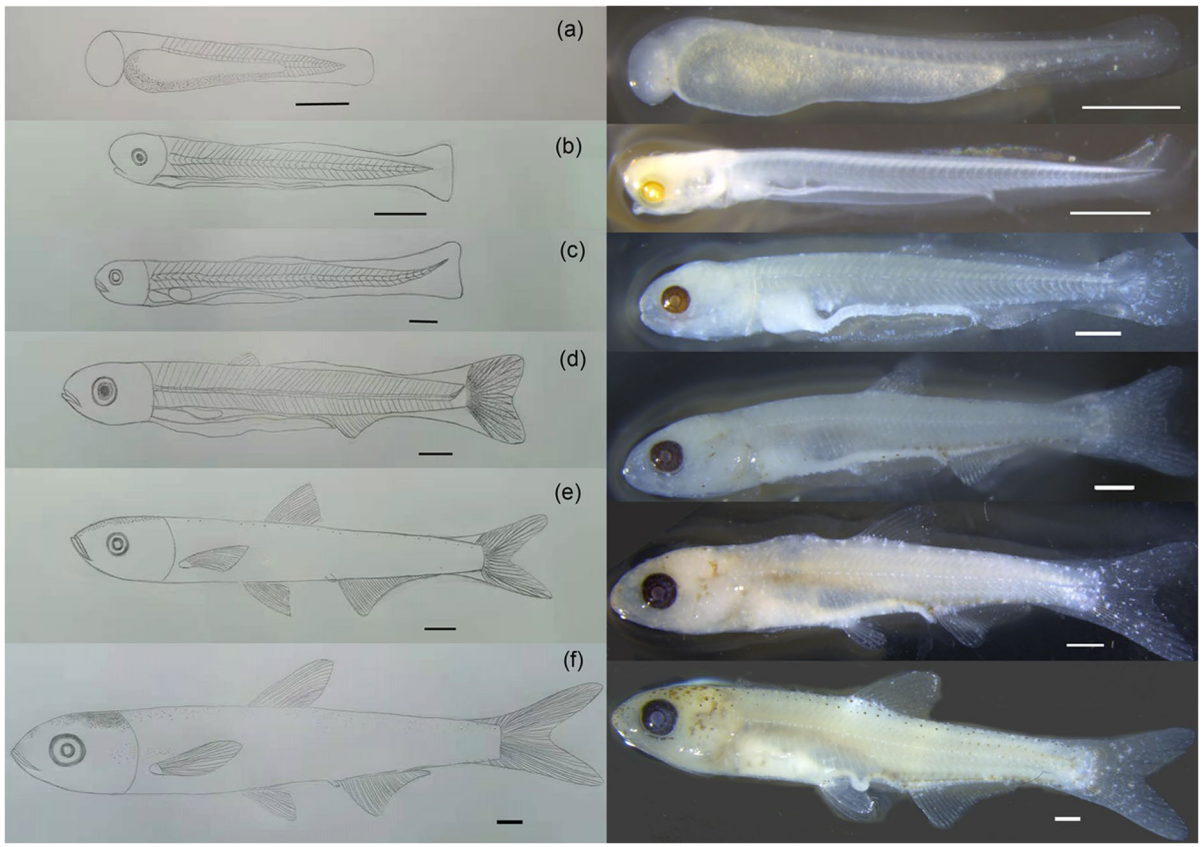

Fig. 2 Early ontogenetic development of *Culter alburnus*. a Newly hatched yolk-sac larvae (5.45 mm *BL*); b preflexion larvae (6.78 mm *BL*); c early flexion larvae (10.07 mm *BL*); d flexion larvae (12.51 mm *BL*); e postflexion larvae (15.01 mm *BL*); f juvenile (18.04 mm *BL*) (scale bars = 1 mm)

was slightly coiled. The mouth was in a terminal position. Internal organs were visible with a paddle-like caudal finfold (Fig. 3). The myomere counts are listed in Table 1.

Flexion stage (Fig. 2c, d)

This stage began with the notochord flexion and ended in flexion completion. The pectoral fin was completely developed, and caudal, dorsal, and anal fin rays developed, with pelvic buds appearing. The finfolds disappeared, and the interior organs were no longer visible (Fig. 3). Predorsal, middle, and postanal myomeres varied between larvae ≤ 11 mm *BL* and larvae > 11 mm *BL* (Table 1). In the later flexion stage, a row of melanophores was observed along the dorsal and ventral margins, and some were scattered on the head.

Postflexion stage (Fig. 2e)

The mouth was in a sub-superior position and the operculum was wholly formed. All fins were wholly formed and further ossified (Fig. 3). At the end of this stage, the total number of fin rays was 14–15 pectoral, 7 dorsal, 8 pelvic, and 22 anal. Pre-anal and postanal myomeres were counted as 19 and 20–22, respectively.

Juvenile stage (Table 1; Fig. 2f)

The body shape began to resemble the adult phenotype. In the dorsal margin of the body, three

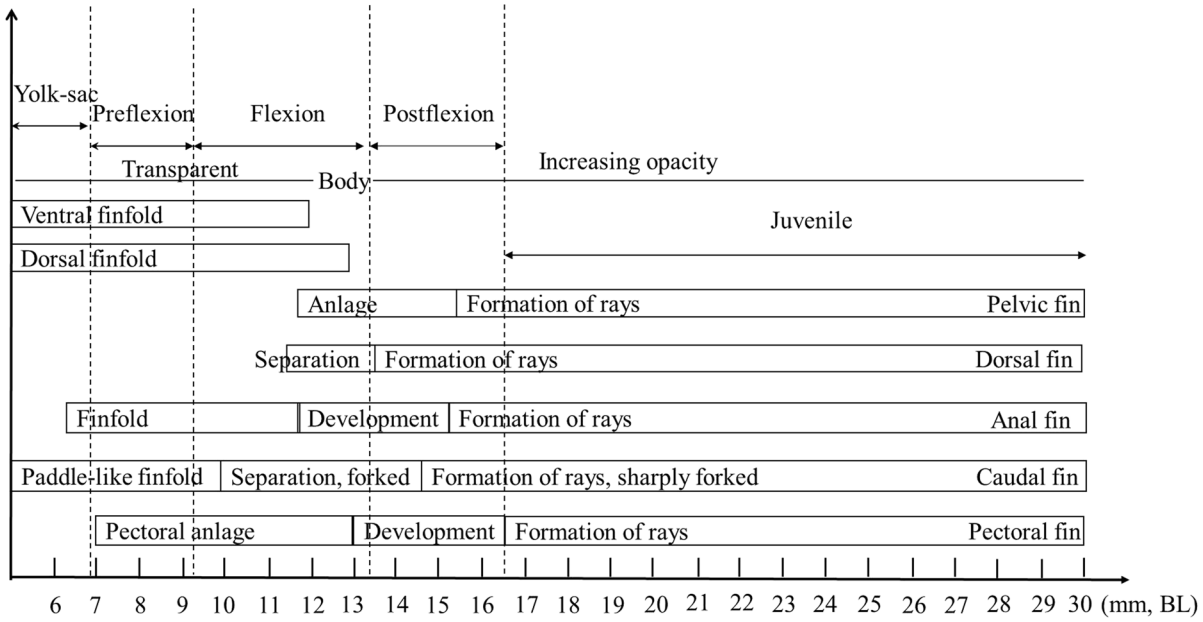

Fig. 3 Morphological events observed during ontogenetic developmental process of *Culter alburnus*

longitudinal bands composed of punctate and floriform chromatophores initially extended from the head to the caudal peduncle. Pigmentations developed toward the abdomen and eventually developed into five longitudinal bands. Dendritic and punctate chromatophores were widely distributed on the head, with intense pigmentation on the back of the head, and snout, and behind the eyes. Some rows of punctate chromatophores were scattered on the caudal fin, dorsal fin, anal fin, and pectoral fin. Pigments were also found along the postmedial line of the body.

The mid-size of stage transition from yolk sac to preflexion was calculated as 6.88 mm *BL*, from preflexion to flexion as 9.10 mm *BL*, from flexion to postflexion as 13.27 mm *BL*, and from postflexion to juvenile as 16.2 mm *BL*.

Morphometric relations

Head length/*BL* continually increased throughout the developmental stages, up to the postflexion stage, and snout length/head length also increased until the juvenile stage. The eye diameter/head length was initially large and increased during the flexion stage. The trunk length/*BL* decreased throughout development, and the dorsal fin and anal fin got closer and closer to the snout. There was little change in the caudal peduncle length/*BL* and pre-pelvic length/*BL* throughout development (Table 1).

Growth pattern

Head length and head height showed positive allometric growth ($b=1.458$ and 1.588, respectively) before the inflection point (13.46 mm) and isometric after it (Fig. 4a, b). The trunk length had negative allometric growth throughout development, while the growth of musculature height was positively allometric ($b=1.89$) before the inflection point (12.18 mm) and then continued with positive, though reduced allometry (Fig. 4c, d). Tail length and caudal peduncle length showed isometric growth before the inflection point (9.79 mm and 12.18 mm, respectively) and positively allometric growth ($b=1.477$ and 1.225) after it (Fig. 4e, f). Body depth growth was positively allometric throughout development ($b=1.249$; Fig. 4g). Finally, the eye diameter showed isometric growth up to the inflection point (14.30 mm) and positive allometric growth after it ($b=1.519$; Fig. 4h).

Otolith shape and microstructure

The sagittal otoliths of newly hatched larva were round until approximately 10.4 (8.89–11.88) mm *BL*,

then became elliptical, and finally became teardrop-shaped with a long, pointed, and fragile posterior end from 11.5 (10.4–12.6) mm *BL* (Fig. 5). On hatching day, the sagittae showed a black primordium in the center, with no increments or bands (Fig. 5a). The first band was observed in the sagittae of 1 dph, with a light zone on the edge of the otolith, formed on the collection day (Fig. 5b). Thus, the first band corresponded to hatching. The first increment, composed of a light zone and a dark zone, was observed in the sagittae of 2 dph larvae; after that, regular increments were deposited in the otoliths. Increments were clear in the round and elliptical sagittae (Fig. 5c–e) and became unclear in teardrop sagittae, with uncountable increments on the rostra (Fig. 5f). The otolith length (*OL*) and otolith width (*OW*) of 147 sagittae ranged from 22.17 to 457.42 μm and from 20.44 to 189.59 μm, respectively.

Lapillar otoliths of newly hatched larvae were slightly oval, showed a black primordium in the center, and had no band or increment (Fig. 6a). The first band was observed in the lapilli of 1 dph larvae, corresponding to hatching (as per the sagittae) (Fig. 6b). No increment or band was formed in the lapilli of 2 and 3 dph, and a light zone followed the hatching band (Fig. 6c). In the lapilli of 4 dph, the second band was observed on the edge of the otolith, corresponding to yolk sac absorption (Fig. 6d). Increments composed of a light zone and a dark zone were deposited following the yolk sac absorption band in the lapilli after 4 dph. The increments were thin and faint during the preflexion and early flexion stages (4 to 16 dph; Fig. 6e) and subsequently increased in width and contrast. Increments were broad and well defined during the postflexion stage (Fig. 6f) and remained regular and visible throughout the juvenile stage (Fig. 6g). After the flexion stage, otoliths became increasingly elliptical with a squarish posterior edge, and the core was offset towards the anterior and ventral edges of the lapillus. The *OL* and *OW* of 203 lapilli ranged from 19.48 to 448.75 μm and 17.76 to 370.53 μm, respectively.

Validating daily periodicity of growth increments in the otoliths

The relationship between the *BL* and the sagittal radius was fitted to a quadratic regression ($r^2 = 0.92$, $F_{3,\ 124} = 8175.5$, $P < 0.01$; Fig. 7a). The sagittal nucleus radius (from the primordium to the hatching band) ranged from 8.10 to 19.46 μm (mean, 16.35 ± 2.86 μm) for 47 hatchery larvae and from 9.18 to 18.40 μm (mean, 11.86 ± 1.24 μm) for 82 experimental larvae. The number of sagittae increments from 113 preflexion and early flexion larvae was counted. The linear relationship between age (*A*) and the number of increments (*N*) in the sagittae was expressed as follows: $A = 0.075 + 1.003\ N$ ($r^2 = 0.997$, $F_{1,\ 112} = 33{,}520$, $P < 0.05$; Fig. 7b). The slope of the linear regression was not significantly different from one (95% CI = 0.99 to 1.02; *t*-test, $t_{113} = 0.6$, $P > 0.05$), confirming daily increment deposition in sagittae. The intercept was 0.075 (95% CI = −0.018 to 0.168), indicating that the first daily increment was formed at 1 dph.

The relationship between *BL* and lapillus radius was fitted to a linear regression ($r^2 = 0.98$, $F_{1,\ 191} = 7650.2$, $P < 0.01$; Fig. 7c). The hatching band in the lapilli of 46 hatchery larvae and 122 experimental larvae had a radius of 12.21 ± 1.89 μm (7.99–15.12 μm) and 10.28 ± 0.97 μm (7.95–12.97 μm), respectively. The radius of the core (from the primordium to the yolk-sac absorption band) in the lapilli of 27 hatchery and 109 experimental larvae was 19.05 ± 1.87 μm (14.13–21.83 μm) and 16.20 ± 1.42 μm (12.89–20.18 μm), respectively. The linear regression between age (*A*) and number of increments (*N*) in the lapilli was fitted by the following: $A = 3.143 + 0.998\ N$ ($r^2 = 0.999$, $F_{1,\ 120} = 270{,}134$, $P < 0.05$; Fig. 7d). The slope of the regression did not differ from one (95% CI = 0.994 to 1.001; *t*-test, $t_{113} = -1.25$, $P > 0.05$). The number of increments differed from the actual age of reared larvae and juveniles by 3.143 (95% CI = 3.045 to 3.241), confirming that growth increments were deposited daily from 4 dph. The mean increment width in the lapilli of experimental larvae gradually increased and reached the broadest at the 21st increment then steadily declined from the 26th increment (Fig. 8).

Discussion

In the present study, morphological characters at each developmental stage were described, diagnostic characteristics (e.g., myomeres, yolk sac shape, fin rays, color patterns, morphometric traits) were provided, and allometric growth patterns were estimated.

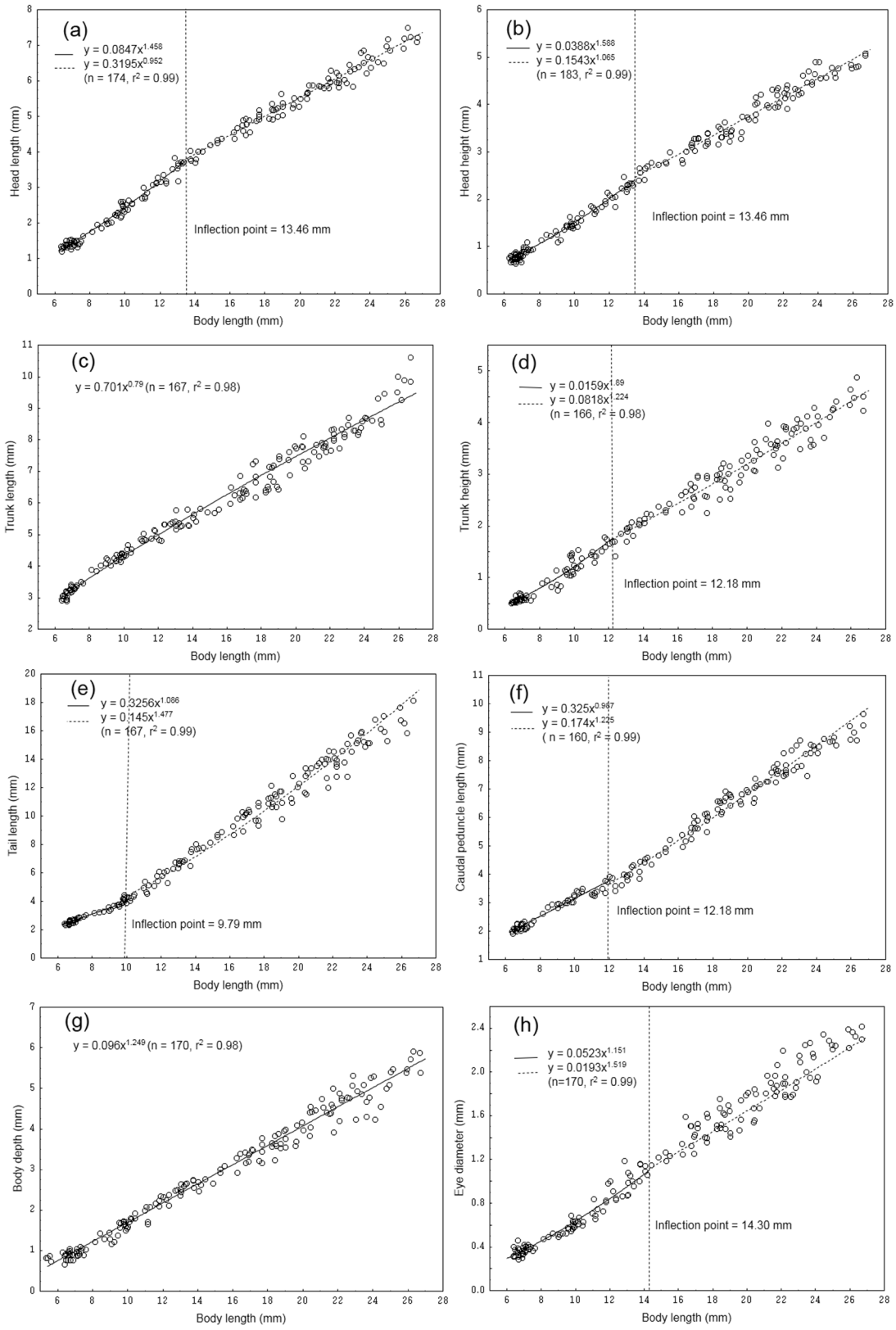
(a)
y = 0.0847x^1.458
y = 0.3195x^0.952
(n = 174, r² = 0.99)
Inflection point = 13.46 mm
Head length (mm)
Body length (mm)
(b)
y = 0.0388x^1.588
y = 0.1543x^1.065
(n = 183, r² = 0.99)
Inflection point = 13.46 mm
Head height (mm)
Body length (mm)
(c)
y = 0.701x^0.79 (n = 167, r² = 0.98)
Trunk length (mm)
Body length (mm)
(d)
y = 0.0159x^1.89
y = 0.0818x^1.224
(n = 166, r² = 0.98)
Inflection point = 12.18 mm
Trunk height (mm)
Body length (mm)
(e)
y = 0.3256x^1.086
y = 0.145x^1.477
(n = 167, r² = 0.99)
Inflection point = 9.79 mm
Tail length (mm)
Body length (mm)
(f)
y = 0.325x^0.987
y = 0.174x^1.225
(n = 160, r² = 0.99)
Inflection point = 12.18 mm
Caudal peduncle length (mm)
Body length (mm)
(g)
y = 0.096x^1.249 (n = 170, r² = 0.98)
Body depth (mm)
Body length (mm)
(h)
y = 0.0523x^1.151
y = 0.0193x^1.519
(n=170, r² = 0.99)
Inflection point = 14.30 mm
Eye diameter (mm)
Body length (mm)

◂ **Fig. 4** Morphometric relationships between body length (*BL*, mm) and **a** head length, **b** head height, **c** trunk length, **d** musculature height, **e** tail length, **f** caudal-peduncle length, **g** body height, **h** eye diameter during the early development of reared *Culter alburnus*

In addition, daily deposition rate of increments was validated and the first increment was observed at 1 dph in sagittal and 4 dph in lapillar otoliths, with the hatching band present in both sagittae and lapilli, and changing increment widths and contrast in lapilli with growth and development.

Ontogenetic development

The ontogenetic development of *C. alburnus* includes three distinct phases. During the first phase (yolk sac and preflexion stages), the mouth and anus opened, the eyes become pigmented, and the intestinal tract and gas bladder develop. During the second phase (flexion stage), fin rays are differentiated and formed and the finfolds are absorbed. Finally, during the third phase (the postflexion and juvenile stages), organs and systems became fully formed, and pigments and melanophores appear and increase in the head and body.

The morphological developmental process of *C. alburnus* mirrors the ontogenetic sequence of other cyprinids (Wan et al. 1999; Yin and Lv 2010). In previous studies, the *C. alburnus* yolk sac depletion at 4 dph was observed in cohorts from Xingkai Lake, Taihu Lake, and Hajiang River, reared in water temperatures 27, 26–31, and 23–25 °C. Moreover, morphological development during the yolk sac stage in this study was also in accordance with previous studies, although the body size at hatching in this study was larger than that in other populations (Gu et al. 2008; Liu et al. 2012; Shao et al. 2016).

In the early stages of life, *C. alburnus* can be distinguished from most species in other genera and families by its yolk sac shape, an oval gas bladder, and the number of myomeres and fin rays (Cao et al. 2007). *Culter alburnus* and its congeners, which are found in the Yangtze River and have available information on their ontogenesis, show similar early development (appearance of eyes, mouth, intestine tract, swimming bladder, and absorption of the yolk sac at 3 or 4 dph). They also have many common characteristics, including rod-like yolk sacs, > 35 total and > 15 postanal myomere counts, and more than 20 anal fin rays (Wan et al. 1999; Li et al. 2005; Yin and Lv 2010; Wang et al. 2020). However, *C. alburnus* can be distinguished from *Ancherythroculter nigrocauda* Yin and Woo 1964, *Sinibrama taeniatus* (Nichols 1941), *Megalobrama skolkovii* (Dybowsky 1872), and *M. pellegrini* (Tchang 1930) by their gas bladder shape and color, myomeres, pigmentation occurrence, and anal fin rays (Wan et al. 1999; Li et al. 2005; Yin and Lv 2010; Wang et al. 2020) (Table 2).

Sympatric species of the same genus *C. dabryi* Bleeker 1871 and *C. mongolicus* (Basilewsky 1855) have similar morphological characteristics during yolk sac stage and a similar yolk sac duration to *C. alburnus*, but no information is available on their ontogenetic development, which prevents comparison with *C. alburnus* in this study (Jiang et al. 2008). In addition to these morphological characters discussed above, morphometric relations, which indicate eye diameter, position of eyes, anus, dorsal fin, anal fin, and pelvic fin, can be used to verify the identification of *C. alburnus* larvae.

The body of a fish can be divided into head, trunk, and tail segments, which play different roles in feeding, locomotion, metabolism, digestion, and respiration and show different allometric growth patterns (Khemis et al. 2013). Head development is vital for feeding and shows prioritized growth in many teleost groups, helping newly hatched larvae establish exogenous feeding (Peña and Dumas 2009; Gao et al. 2015). Head length and depth of *C. alburnus* showed positive allometric growth patterns from hatching until the late flexion stage, implying differentiation and development of neural (midbrain and hindbrain) and sensorial structures (free neuromasts, vision, and olfaction), respiratory systems (branchial apparatus), and food processing organs (mouth, hyoid, and mandibular structures). The development of these organs and systems allows larvae to react to light stimuli, find and obtain prey, detect potential predators, and successfully complete the transition from endogenous to exogenous nutrition. This facilitates a higher growth rate and better survival probability during the early stages of life history (Gisbert et al. 2002; Peña and Dumas 2009; Wang et al. 2019).

Trunk growth can be related to the development of myomeres, vertebral columns, digestive tracts and associated glands, which assist with locomotion and metabolism (Gao et al. 2015; Saemi-Komsari et al.

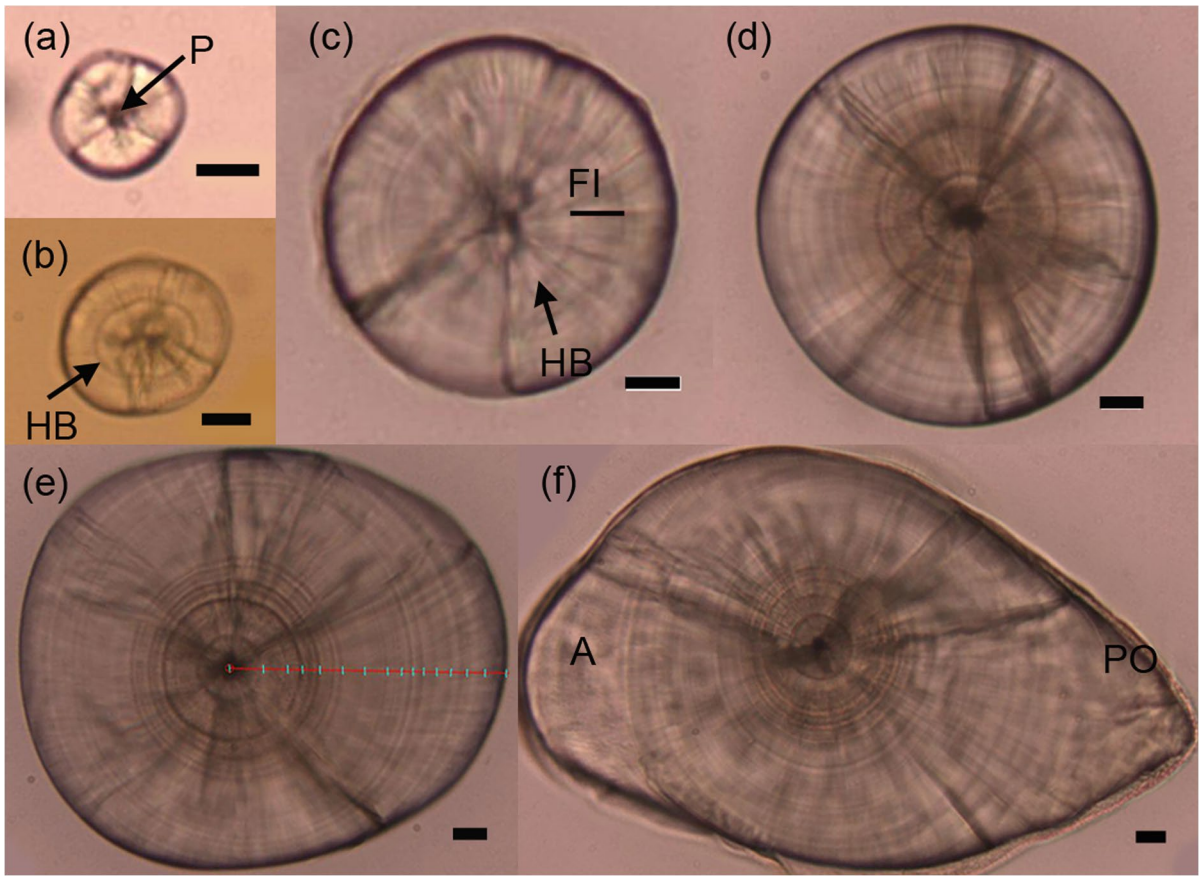

Fig. 5 Sagittal otoliths of reared larval *Culter alburnus*. **a** The circular otolith of newly hatched larva with 5.20 mm *BL*; **b** the circular otolith of larva 1 day post hatch (dph) with 5.61 mm *BL*; **c** the circular otolith of larva 2 days dph with 7.05 mm *BL*; **d** the circular otolith of larva 7 days dph with 8.15 mm *BL*; **e** the elliptical otolith of larva 13 days dph with 10.21 mm *BL*, red line shows the radius and the direction of increment counting and measurement on the posterior area; **f** the tear-drop-shaped otolith of larva 13 days dph with 11.18 mm *BL*. P, primordium; HB, the hatching band; FI, the first increment; A and PO indicate the anterior and posterior area of the otoliths, respectively (scale bars = 10 microns)

2018). In the trunk segment of *C. alburnus*, trunk length showed negative allometric growth throughout development, while musculature height had positive allometric growth until the flexion stage. The rapid growth of musculature height implies continuous development of the digestive tract and glands (i.e., formation of kidney and mucosa folds and coiling of the intestine), promoting enzymatic activities and enhancing digestive and assimilative abilities (Peña and Dumas 2009; Xu et al. 2020). The negative allometric growth of trunk length may be related to the larval anguilliform swimming style, which mainly depends on the body finfold (Saemi-Komsari et al. 2018). The allometric growth pattern on the trunk segment in this study has also been observed in many fish species, such as the American shad *Alosa sapidissima* (Wilson 1881), spotted sand bass *Paralabrax maculatofasciatus* (Steindachner 1868), and electric yellow cichlid *Labidochromis caeruleus* Fryer 1956 (Peña and Dumas 2009; Gao et al. 2015; Saemi-Komsari et al. 2018).

Tail growth can enlarge the propulsive area and promote propulsive power, assisting with locomotor function and swimming mode (Khemis et al. 2013). The tail length and caudal peduncle length of *C. alburnus* displayed negative allometric growth until the flexion stage. Faster tail growth after the flexion stage, coupled with the development of paired and unpaired fins and eyes, and the absorption of the body finfold may prompt a progressive transition of

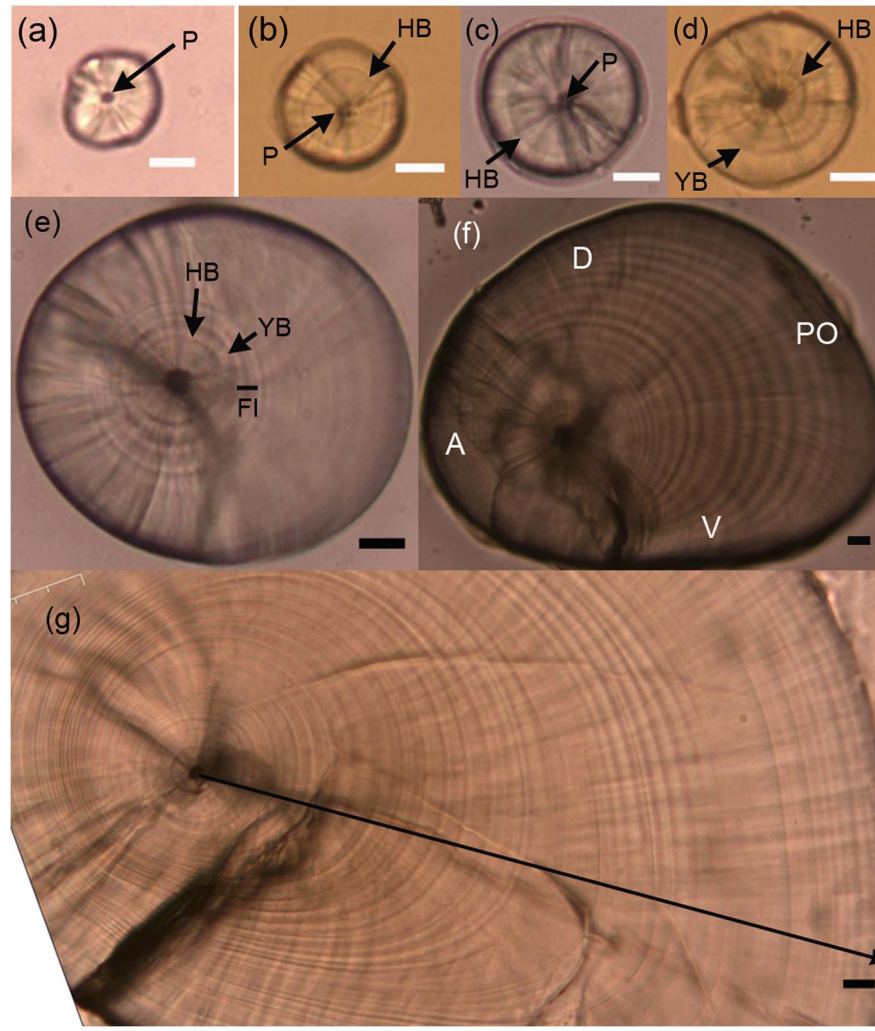

Fig. 6 Lapillar otoliths of reared larval and juvenile *Culter alburnus*. **a** The oval lapillus of newly hatched larva with 5.44 mm *BL*; **b** the lapillus of yolk-sac larva 1 day post hatch (dph) with 5.61 mm *BL*; **c** the lapillus of preflexion larva 3 dph with 6.47 mm *BL*; **d** the lapillus of preflexion larva 4 dph with 7.46 mm *BL*; **e** the oblong lapillus of flexion larva 14 dph with 10.78 mm *BL*; **f** the lapillus of post-flexion larva with 15.78 mm *BL*; **g** the posterior area in the lapillus of a juvenile with 22.15 mm *BL*, solid arrow indicates the radius and the direction of increment counting and measurement. P, primordium; HB, the hatching band; YB, the yolk-sac absorption band; FI, the first increment; A, PO, D, and V indicate the anterior, posterior, dorsal, and ventral areas of the otoliths, respectively (scale bars = 10 microns)

larval swimming modes from anguilliform swimming to subcarangiform swimming (Khemis et al. 2013; Saemi-Komsari et al. 2018). Subcarangiform swimming leads to higher efficiency and speed, which greatly improves the ability to seek and capture prey and avoid predators (Khemis et al. 2013). Fast tail growth during the later flexion stages has been observed in other species, such as the spotted seahorse *Hippocampus kuda* Bleeker 1852, mandarin fish *Siniperca chuatsi* (Basilewsky 1855), where the tail may play a minor locomotory role during early larval stages (Choo and Liew 2006; Song et al. 2019; Xu et al. 2020). In contrast, many fish species show fast early tail growth, indicating that allometric growth patterns during early ontogenetic development are specific-species and based on the immediate needs of each stage (Peña and Dumas 2009; Saemi-Komsari et al. 2018; Wang et al. 2019).

Validation of otolith increments

Sagitta and lapillus are the most commonly used otoliths to estimate age and growth of fish (Morioka et al. 2006; Joh et al. 2011; Song et al. 2019). In cyprinid fish, lapilli maintain a regular shape throughout development and are suitable to determine age, whereas sagittae show visible and countable increments during initial stages, but increments become uncountable and fragile when sagittae develop a teardrop shape.

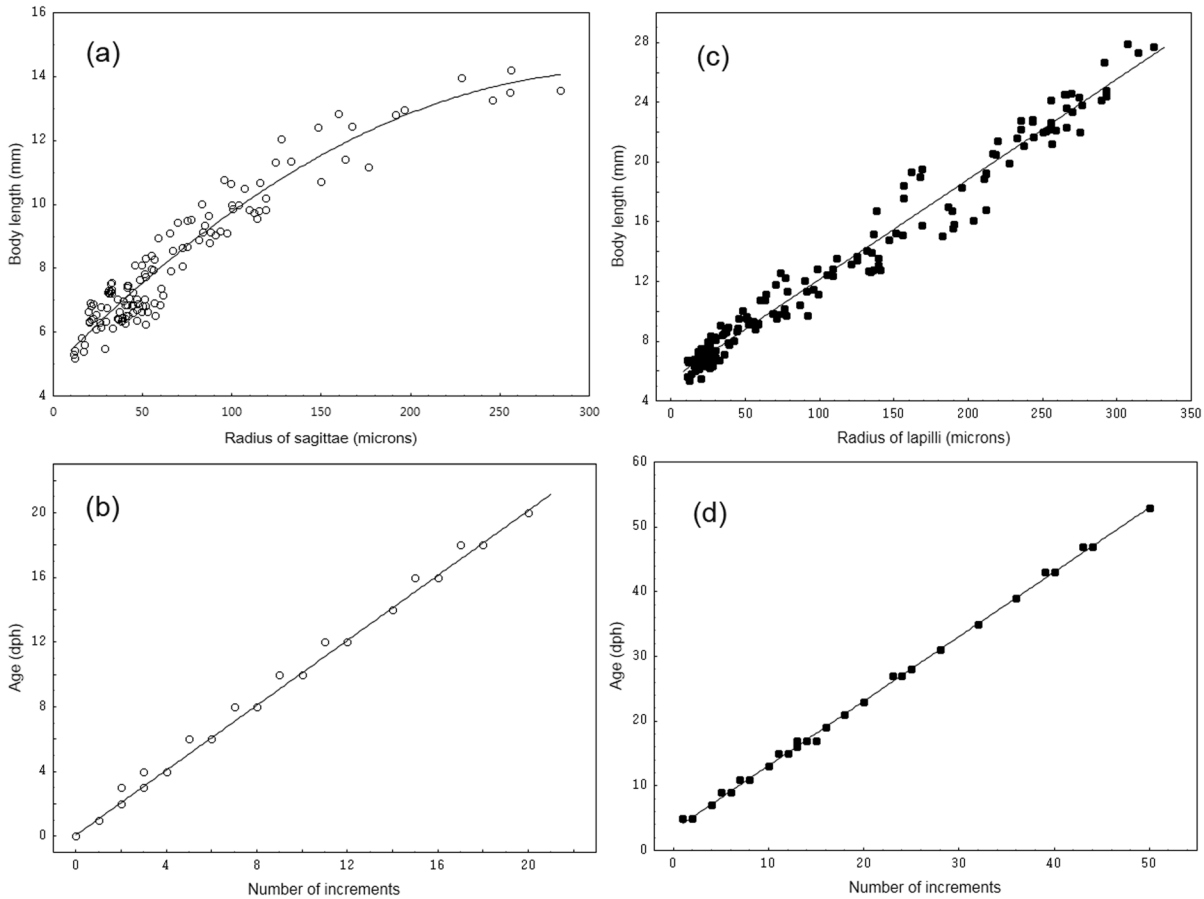

Fig. 7 Relationship between body length (mm) and radius of sagittae (**a**) and lapilli (**b**) of hatchery and experimental larvae of *Culter alburnus* was fitted by the following: $y=4.871+0.058x-9.026\times10^{-5}x^2$ ($n=127$, $r^2=0.92$) and $y=5.45+0.067x$ ($n=193$, $r^2=0.98$), respectively, and relationship between age, the number of days post hatch (dph), and the number of increments in sagittae (**c**) and lapilli (**d**) of hatchery and experimental larvae was fitted by the following: $y=0.075+1.003x$ ($n=113$) and $y=3.143+0.998x$ ($n=122$), respectively

Sagittae of many cyprinid fish have clear increments until the later flexion stage or later at 20–30 dph or more, such as, *A. nigrocauda* (18 dph), *Hemigrammopetersius barnardi* (Here 1936) (20–30 dph), and European chub *Squalius cephalus* (Linnaeus 1758; about 45 dph) (Morioka et al. 2006; Li 2008; Bounket et al. 2019). Similar to other cyprinids, the sagitta of *C. alburnus* showed visible increments up to the late flexion stage at 12–20 dph.

Cyprinids are the most common freshwater fish in China, and studies have established the daily deposition rate in some species' sagittae and lapilli (Fu et al. 2003; Yan et al. 2017; Boumket et al. 2019). However, few validation studies have been conducted on *Culter* spp., which include many widely distributed and commercially important fish species (Li 2008). Our study confirmed that increment deposition occurred daily in the sagitta and lapillus of *C. alburnus*, consistent with the situation in other cyprinid fish (Ding et al. 2015; Huang et al. 2017; Yan et al. 2017). However, the daily periodicity of increment formation in *C. alburnus* otoliths occurs under normal environmental conditions and may not be valid if fish are subjected to extreme water temperatures or starvation.

The relationship between actual age and increment counts suggested that the first daily increment was formed on the 1st and 4th day in the sagittae and lapilli of *C. alburnus,* respectively. Observations of the otolith microstructure showed that a hatching band

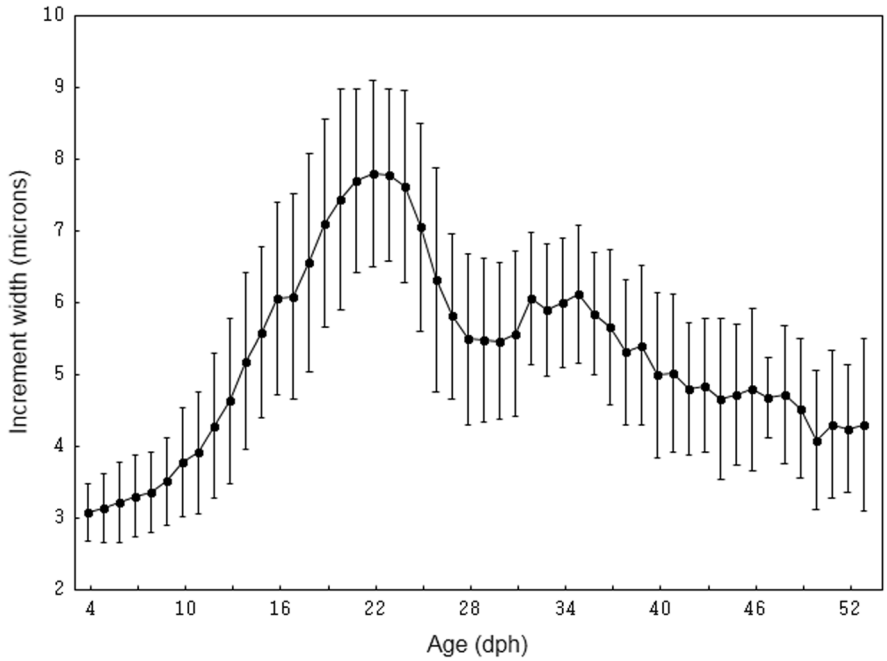

Fig. 8 Mean ± standard deviation increment widths in the lapilli of experimental larvae of *Culter alburnus*

Table 2 Morphological characteristics, which can be used to identify *Culter alburnus* from its congeners: *Ancherythroculter nigrocauda*, *Sinibrama taeniatus*, *Megalobrama skolkovii*, and *M. pellegrini* in early life history

Species	*C. alburnus*	*A. nigrocauda*	*S. taeniatus*	*M. skolkovii*	*M. pellegrini*
Size at hatch (mm)	5.56–5.85	4.10 ± 0.02	4.54 ± 0.04	4.3	4.75–4.9
Gas bladder	Oval, colorless	Elliptical, colorless	Elliptical, black	Oval, black	Oval, black
Myomeres	39–43	42–47	37–40	38–49	43–48
Middle/postanal myomeres	11–13, 16–18	–	–	12–13, 16–17	16, 18
Occurrence of pigments	Postflexion	Flexion	Yolk-sac	Postflexion	Preflexion
Anal fin rays	23–25	25–26	23	25–27	25–27

was present in both sagittae and lapilli. Clear daily increments were formed following the hatching band on the sagittae but did not occur on the lapilli until the 4th day. Both methods documented that the hatching bands on the sagittae and lapilli were observed the 1st day, which occur in many cyprinid fish, e.g., *A. nigrocauda*, *S. cephalus*, *Schizothorax* (*Racoma*) *davidi* (Sauvage 1880), and *Tanichthys albonubes* Lin 1932 (Shi et al. 2006; Li 2008; Yan et al. 2017; Boumket et al. 2019). However, *C. alburnus* lapilli displayed the first increment on the 4th day, corresponding to yolk sac absorption, and no discernible increment occurred during the yolk sac stage. Deposition of the first increment at yolk sac absorption or the first feeding has been reported in some cyprinid fish (e.g., mud carp *Cirrhinus molitorella* (Valenciennes 1842)), and many species from other families, such as *Pseudopleuronectes herzensteini* (Jordan et Snyder 1901), *S. chuatsi*, and *Coilia ectenes* (Jordan et Seale 1905) (Joh et al. 2011; Huang et al. 2014; Song et al. 2019). A hatching band has been observed in the otoliths of all studied cyprinid fish and is also common in other species, such as *Siganus spinus* (Linnaeus 1758), mackerel icefish *Champsocephalus gunnari* Lönnberg 1905, and *Lophius budegassa* (Spinola 1807) (Soliman et al. 2010; Mesa et al. 2013; Hernández et al. 2015). The yolk sac band, which formed in the lapilli of *C. alburnus*, has also been observed in the otoliths of some other cyprinids, including *A. nigrocauda*, *T. albonubes*, and *C. molitorella* (Shi et al.

2006; Li 2008; Huang et al. 2017) and other fish species, for example, *P. herzensteini* and *L. budegassa* (Joh et al. 2011; Herńandez et al. 2015).

Increment patterns usually show various contrasts and widths at different developmental stages due to ontogenetic, physiological, and genetic factors (Bounket et al. 2019; Huang et al. 2017; Marannu et al. 2017). In this study, the lapillus increments were thin and faint during the preflexion and early flexion stages and increased in contrast and width to reach a maximum during the postflexion stage. Thin and obscure increments near the core have also been observed in many fish species, such as *C. molitorella*, *Lateolabrax japonicus* (Cuvier 1828), and *S. spinus* and *P. herzensteini* (Islam et al. 2009;Soliman et al. 2010; Joh et al. 2011; Huang et al. 2017). Increment patterns in the central area may be related to weak swimming ability, narrow activity range, stable environmental conditions, and slow growth of newly hatched larvae. Increment width and contrast reach their maxima at the postflexion stage, when the swimming mode changes and the ontogenetic diet and habitat shifts occurred, allowing larvae to have a wide range of action, intense activity, and the ability to feed on plentiful prey. As a result, fish undergo variable environmental conditions and grow faster, which may explain the occurrence of the increments with the strongest contrast and broadest widths (Green et al. 2009). For example, the increment widths of *C. molitorella* and black-spot tuskfish *Choerodon schoenleinii* (Valenciennes 1839) reached the maximum value, and *C. molitorella* showed the clearest increments during the metamorphosis period (Yamada et al. 2009; Huang et al. 2017). In other species, metamorphosis can be recorded in otoliths by microstructural characteristics, such as accessory primordia, wide and obscure increments, or considerably reduced increment widths (Soliman et al. 2010; Joh et al. 2011; Song et al. 2019). The observed patterns in this study of increment widths, showing an increasing trend followed by a steady decrease, are common in other species, such as *L. budegassa*, *C. molitorella*, and *C. schoenleinii* (Yamada et al. 2009; Hernàndez et al. 2015; Huang et al. 2017).

Sagittae of Cyprinidae, Pleuronectids, and Perciformes are considered unsuitable for increment analysis because of their complicated and irregular morphology with accessory primordia and an elongated posterior rostrum after metamorphosis (Joh et al. 2011; Bounket et al. 2019; Song et al. 2019). This study showed that increments were not sufficiently clear around the centrum and were too narrow to distinguish in the lapilli, but increment widths in sagittae were large and clear during the early larval stage. Therefore, we suggest that increment counts of sagittae can be used in teardrop-shaped sagittae in cases where increments in the central region of lapilli are difficult to discern. Similarly, it is also suggested that both the sagittal and lapillus otoliths of the same individual should be used to estimate age in *P. herzensteini* and *L. japonicas* (Islam et al. 2009; Joh et al. 2011).

In this study, hatchery-reared *C. alburnus* larvae had a higher growth rate than experimentally reared individuals, with hatchery larvae showing growth rates similar to those reported by Gu et al. (2008). Differences in growth rate between the hatchery and the experimental tanks may be explained by prey nutrition and habitat space, as the abiotic factors were similar between the two rearing systems. The radii of hatching and yolk sac bands were also larger in hatchery larvae than in experimental larvae, indicating that otoliths grew faster in hatchery larvae than in experimental larvae. Consequently, the duration of each developmental stage was longer in experimentally reared larvae, so body size is an important standard for defining developmental stages.

This study lays a solid foundation for the aquaculture industry and studying early-life ecology of *C. alburnus*. It provided:

- Morphological characters and morphometric relations that allow the identification of *C. alburnus* larvae collected in the field
- Information on ontogenetic development and allometric growth patterns
- Validation of daily increments in sagittal otoliths that allow accurate age estimation in larvae
- Information on the relationship between otolith microstructure patterns and larval development stages

Acknowledgements We express sincere thanks to the Dongting Lake Fish Breeding Farm for providing specimens.

Author contribution Huang conceived the ideas and designed the methodology; Huang, Deng, Wang, and Shen collected the data and analyzed the data; Huang, Song, and Liu led

the writing of the manuscript; all authors contributed critically to the drafts and gave final approval for publication.

Funding This research was supported by the National Nature Science Foundation of China by the Young People Grant program (32002394) and Education Department of Hunan Province by the Outstanding Young People Grant program (20B403).

Data availability The datasets generated during and/or analyzed during the current study are available from the corresponding author on reasonable request.

Declarations

Ethical approval The present study complied with current animal laws in China.

Competing interests The authors declare no competing interests.

References

Aldanondo N, Cotano U, Etxebeste E, Irigoien X, Álvarez P, Murguía AMD, Herrero DL (2008) Validation of daily increments deposition in the otoliths of European anchovy larvae (*Engraulis encrasicolus* L.) reared under different temperature conditions. Fish Res 93:257–264

Belchier M, Lawson J (2013) An analysis of temporal variability in abundance, diversity and growth rates within the coastal ichthyoplankton assemblage of South Georgia (sub-Antarctic). Polar Biol 36(7):969–983

Beveren EV, Klein M, Serrão EA, Gonçalves EJ, Borges R (2016) Early life history of larvae and early juvenile Atlantic horse mackerel *Trachurus trachurus* off the Portuguese west coast. Fish Res 183:111–118

Bounket B, Gibert P, Gennotte V, Argillier C, Carrel G, Maire A, Logez M, Morat F (2019) Otolith shape analysis and daily increment validation during ontogeny of larval and juvenile European chub *Squalius cephalus*. J Fish Biol 95(2):444–452

Cao W, Chang J, Qiao Y, Duan Z (2007) Fish resources of early life history stages in Yangtze River. Water Power Press, Beijing

Chiu YW, Tso CW, Shieh BS, Liu CC, Lin YS, Liang SH (2012) Evaluation of the predatory effects of an introduced fish, *Culter alburnus*, on the fish community in a small stream of northern Taiwan. Zool Stud 51(8):1438–1445

Choo CK, Liew HC (2006) Morphological development and allometric growth patterns in the juvenile seahorse *Hippocampus kuda* bleeker. J Fish Biol 69(2):426–445

Ding C, Chen Y, He D, Tao J (2015) Validation of daily increment formation in otoliths for *Gymnocypris selincuoensis* in the Tibetan Plateau, China. Ecol Evol 5:3243–3249

Dong XS, Meng QL, An L, Wang XR, Liu YQ, Zhao B, Zhang GX, Chen P (2017) Observation on embryonic development of the topmouth culter (*Culter alburnus* Basilewsky) of Huanghe River. J Yangtze Univ (Natural Science Edition) 14:36–39+4 (in Chinese, with English abstract)

Dos Santos JA, Soares CM, Bialetzki A (2020) Early ontogeny of yellowtail tetra fish *Astyanax lacustris* (Characiformes: Characidae). Aquac Res 51:4030–4042

Fu C, Wu J, Chen J, Wu Q, Lei G (2003) Freshwater fish biodiversity in the Yangtze River basin of China: patterns, threats and conservation. Biodivers Conserv 12:1649–1685

Gao XQ, Hong L, Liu ZF, Guo ZL, Wang YH, Lei JL (2015) The study of allometric growth pattern of American shad larva and juvenile (*Alosa sapidissima*). Acta Hydrobiol Sin 39:638–644 (in Chinese, with English abstract)

Geffen AJ (1982) Otolith ring deposition in relation to growth rate in herring (*Clupea harengus*) and turbot (*Scophthalmus maximus*) larvae. Mar Biol 71(3):317–326

Gisbert E, Merino G, Muguet JB, Bush D, Piedrahita RH, Conklin DE (2002) Morphological development and allometric growth patterns in hatchery-reared California halibut larvae. J Fish Biol 61:1217–1229

Green BS, Mapstone BD, Carlos G, Begg GA (2009) Tropical fish otoliths: information for assessment, management and ecology. Springer, Dordrecht

Gu Z, Zhu J, Jia Y, Pan Y, Huang X, Xu G, Yang Y (2008) Research on embryonic and postembryonic development of *Erythroculter ilishaeformis* Bleeker of Taihu Lake. J Fish Sci China 15:204–211

Hare JA, Cowen RK (1994) Ontogeny and otolith microstructure of bluefish *Pomatomus saltatrix* (Pisces: Pomatomidae). Mar Biol 118(4):541–550

Hernández C, Landa J, Barrado J, Antolínez A, Santos MB (2015) First estimates of age and growth of juvenile black anglerfish (*Lophius budegassa*), in north-eastern Atlantic waters. Fish Res 161:269–272

Houde ED (1987) Fish early life history dynamics and recruitment variability. Am Fish Soc Symp 2:17–29

Huang YF, Cheng F, Murphy BR, Xie S (2014) Sagittal otolith microstructure and early growth and development of *Coilia ectenes* in the Yangtze Estuary, China. Fish Sci 80:435–443

Huang Y, Chen F, Tang W, Lai Z, Li X (2017) Validation of daily increment deposition and early growth of mud carp *Cirrhinus molitorella*. J Fish Biol 90:1517–1532

Huang YF, Duan GQ, Peng LP (2019) Reviews on the resource status and biological characteristics of *Culter alburnus*. J Anhui Agric Sci 47(19):10–13

Islam MS, Ueno M, Yamashita Y (2009) Otolith microstructure of Japanese sea bass larvae and juveniles: interpretation and utility for ageing. J Appl Ichthyol 25:423–427

Jiang HF, Geng LW, Tong GX, Li CY, Wang SZ, Xu W (2008) Artificial propagation and observation of embryonic and postembryonic development in pond-farmed Mongolian *Culter Erythrocultermongolicus* collected from Jingpo Lake. Fish Sci 35:130–135 (In Chinese, with English abstract)

Joh M, Matsuda T, Satoh N, Tanak N, Ueda Y (2011) Otolith microstructure of brown sole *Pseudopleuronectes herzensteini*: validation of daily ring formation and the occurrence of microstructure denoting metamorphosis. Fish Sci 77:773–783

Khemis IB, Gisbert E, Alcaraz C, Zouiten D, Masmoudi AS, Cahu C (2013) Allometric growth patterns and development in larvae and juveniles of thick-lipped grey mullet *Chelon labrosus* reared in mesocosm conditions. Aquac Res 44:1872–1888

Koumoundouros G, Divanach P, Kentouri PD (1999) Ontogeny and allometric plasticity of *Dentex dentex* (Osteichthyes: Sparidae) in rearing conditions. Mar Biol 135:561–572

Li WJ, Wang JW, Tan DQ, Dan SG (2005) Observation on postembryonic development of *Megalobrama pellegrini*. J Fish China 29:729–736 (in Chinese, with English abstract)

Li Z (2008) Studies on otolith microstructure of larval and juvenile *Ancherythroculter nigrocauda.* Dissertation, Sichuan Agricultural University

Liu DY, Si LN, Zhang XG, Yin HF (2012) Research on embryonic and larvae development of *Culter alburnus* of Xingkai Lake. J Northeast Agric Univ 43:110–116 (in Chinese, with English abstract)

Marannu S, Nakaya M, Takatsu T, Takabatake SI, Joh M, Suzuki Y (2017) Otolith microstructure of arabesque greenling *Pleurogrammus azonus*: a species with a long embryonic period. Fish Res 194:127–134

Mesa ML, Catalano B, Koubbi P, Jones CD (2013) Early ontogeny of the mackerel icefish, *Champsocephalus gunnari*, in the southern Scotia Arc. Polar Biol 36(6):797–805

Miller BS, Kendall AW (2009) Early life history of Marine Fishes. University of California Press

Morioka S, Matsumoto S, Kaunda E (2006) Otolith features and growth of Malawian characid *Hemigrammopetersius barnardi* from the southwestern coast of Lake Malawi. Ichthyol Res 53(2):143–147

Peña R, Dumas S (2009) Development and allometric growth patterns during early life stages of the spotted sand bass *Paralabrax maculatofasciatus* (Percoidei: Serranidae). Sci Mar 2009:183–189

Rocha MSA, Silva RC, Santos JCE, Schorer M, Nascimento MP, Pedreira MM (2020) Comparative larval ontogeny of two fish species (Characiformes and Siluriformes) endemic to the São Francisco River in Brazil. J Fish Biol 96:49–58

Saemi-Komsari M, Mousavi-Sabet H, Kratochwil CF, Sattari M, Eagderi S, Meyer A (2018) Early developmental and allometric patterns in the electric yellow cichlid *Labidochromis caeruleus*. J Fish Biol 92(6):1888–1901

Sanjarani VN, Reza EH, Mojtaba M, Bettina R (2018) Early otolith development in the critically endangered toothcarp, *Aphanius farsicus* (Teleostei: Cyprinodontidae). Environ Biol Fish 101:1–9

Sarpédonti V, Ponton D, Ching CV (2000) Description and ontogeny of young *Stolephorus baganensis* and *Thryssa kammalensis*, two Engraulididae from Peninsular Malaysia. J Fish Biol 56:1460–1476

Shao JC, Liu CL, Qin F, Qin CJ, Gu ZM (2016) Observation on embryonic and larval development of *Culter alburnus* of Hanjiang River. J Huazhong Agric Univ 35:111–116 (in Chinese, with English abstract)

Shi F, Sun J, Lin XT, Liu HS (2006) Otolith ontogeny and increment formation in larval *Tanichthys albonubes*. Chin J Zool 41:10–16 (in Chinese, with English abstract)

Shoji J, Tanaka M (2007) Density dependence in post-recruit Japanese seaperch *Lateolabrax japonicas* in the Chikugu River. Mar Ecol Prog Ser 334:225–262

Soliman VS, Yamada H, Yamaoka K (2010) Early life-history of the spiny siganid *Siganus spinus* (Linnaeus 1758) inferred from otolith microstructure. J Appl Ichthyol 26:540–545

Song Y, Cheng F, Zhao S, Xie S (2019) Ontogenetic development and otolith microstructure in the larval and juvenile stages of mandarin fish *Siniperca chuatsi*. Ichthyol Res 66:57–66

Snik GMJV, Boogaart JGMVD, Osse J (1997) Larval growth patterns in *Cyprinus carpio* and *Clarias gariepinus* with attention to finfold. J Fish Biol 50:1339–1352

Takahashi M, Watanabe Y (2004) Growth rate-dependent recruitment of Japanese anchovy *Engraulis japonicas* in the Kuroshio-Oyashio transitional waters. Mar Ecol Prog Ser 266:227–238

Wan CY, Lin YT, Huang DM (1999) Postembryonic Development of *Megalobrama skolkovii*. J Lake Sci 11:357–362 (in Chinese, with English abstract)

Wang XL, Wen HS, Zhang MZ, Li JF, Fang X, Zhang KQ, Liu Y, Tian Y, Chang ZC, Wang Q (2019) Studies on allometric growth pattern of cultured *Lateolabrax maculatus* larvae during early development. Periodical Ocean Univ China 49:25–30 (in Chinese, with English abstract)

Wang YL, Liu Y, Tian JJ, Yin M, Cai RY, Wang ZJ (2020) Growth and morphological development of larval and juvenile *Sinibrama taeniatus*. Prog Fish Sci 41:58–67 (in Chinese, with English abstract)

Xu B, Wang N, Wei KJ, Zhu XY, Xu J, Ma BS (2020) Allometric growth pattern of *Schizothorax waltoni* Regan at larvae and juvenile stages. J Shanghai Ocean Univ. https://doi.org/10.12024/jsou.20190902795 (in Chinese, with English abstract)

Yamada H, Chimura M, Asami K, Sato T, Kobayashi M, Nanami A (2009) Otolith development and daily increment formation in laboratory-reared larval and juvenile black-spot tuskfish *Choerodon schoenleinii*. Fish Sci 75(5):1141–1146

Yan T, Hu J, Cai Y, Xiong S, Yang S, Wang X, He Z (2017) Otolith development in larval and juvenile *Schizothorax davidi*: ontogeny and growth increment characteristics. Chin J Oceanol Limn 35(5):1197–1204

Yin HC, Lv HY (2010) Growth and development of larva, *Ancherythroculter nigrocauda* Yih et Woo. J Aqua 31:40–42

Yin JS, Xia CZ, Xu W, Kuang YY, Cao DC (2004) Population change of *Culter alburnus* in Xingkai Lake. Acta Hydrobiol Sin 28:490–495 (in Chinese, with English abstract)

Zhu QG, Wang J, Yang SR, Gao X, Cao WX (2015) The daily age and the growth of *Culter alburnus* juveniles at early developmental stages in the Mudong Section of the Three Gorges Reservoir. Acta Hydrobiol Sin 39:983–988 (in Chinese, with English abstract)